Pergamon

Journal of Structural Geology, Vol. 16, No. 5, pp. 677 to 691, 1994

0191-8141/94 $07.00+0.00

Structure, magnetic fabric and emplacement of the Archean Lebel Stock, SW Abitibi Greenstone Belt

ALEXANDER R. CRUDEN and PATRICK LAUNEAU

Tectonic Studies Group, Department of Geology, University of Toronto, Mississauga, Ontario, Canada L5L 1C6

(*Received* 4 *August* 1992; *accepted in revised form* 25 *June* 1993)

Abstract—The anisotropy of magnetic susceptibility (AMS) has been determined in a suite of samples from the *ca* 2680 Ma old, sub-circular, syenitic Lebel Stock which is bound to the north by a major late-Archean shear zone (Larder Lake–Cadillac deformation zone; LCDZ). The AMS defines a magnetic foliation which is parallel to a strong, planar preferred mineral orientation fabric considered to have been acquired during flow of a crystal-laden magma during emplacement. The geometry of the foliation indicates that the stock has an horizontal dish shape at depth. The syenites also contain a well defined magnetic lineation which consistently points toward the LCDZ apart from localities in the south where it trends E–W, parallel to the stock's margin. AMS ellipsoids are dominantly of oblate type except in samples showing solid-state strain and alteration overprints, which often have plane to prolate ellipsoids. The intensity of the magnetic fabric shows a weak spatial variation, being strongest at the southern margin. The magnetic and magmatic fabric pattern, AMS parameter variation and the sense of displacement of the western wall-rocks are used to propose an emplacement mechanism involving southward migration of a relatively thin sheet of syenitic magma from a linear source corresponding to the present location of the LCDZ.

INTRODUCTION

SINCE the work of Graham (1954), Stacey (1960) and Uyeda *et al.* (1963) measurement of the anisotropy of magnetic susceptibility (AMS) of rocks has become an established method for petrofabric analysis (e.g. see reviews by Hrouda 1982, Borradaile 1988). Because the method is sensitive to low percentage anisotropies it is particularly well suited for mapping emplacement-related foliations and lineations in igneous intrusions (e.g. King 1966, Van der Voo & Klootwijk 1972, Ellwood & Whitney 1980, Guillet *et al.* 1983) which are often difficult to determine in the field. Furthermore, the systematic variations of the shape and intensity of the susceptibility ellipsoid observed within some plutons (e.g. Cogné & Perroud 1988, Bouchez *et al.* 1990) can yield important information on the kinematics of magma emplacement.

This paper presents results of a combined structural/AMS study of the Lebel Stock, a sub-circular, 6 km wide, syenitic pluton in the Kirkland Lake area of the Abitibi Greenstone Belt (AGB) of northern Ontario (Fig. 1). The stock is one of many 2.69–2.67 Ga old intrusions which are spatially associated with several major, E–W-trending gold-bearing, crustal-scale deformation zones which characterize the structure of the southern AGB (Dimroth *et al.* 1983a, Colvine *et al.* 1988). The Lebel Stock is particularly interesting because it abuts the Larder Lake–Cadillac deformation zone (LCDZ, Fig. 1) and therefore presents an opportunity to determine: (1) the relative timing between late Archean magmatism and displacements associated with E–W-trending deformation zones; and (2) the relationship between magma emplacement and the structural development of these zones.

GEOLOGICAL SETTING

Regional geology

The 2.75–2.67 Ga old Abitibi Greenstone Belt (Fig. 1), located in the southeastern part of the Superior Province of the Canadian Shield, is the largest single continuous Archean greenstone belt in the world (Windley 1984). The principal lithological subdivisions of the southern AGB proposed by Jackson & Fyon (1991) are summarized in Fig. 1. Following Dimroth *et al.* (1983b) they favour a four-stage plate-tectonic model to interpret Abitibi geology: (1) formation of submarine oceanic (mafic–ultramafic, tholeiitic–komatiitic volcanics) and island-arc (intermediate-felsic, calc-alkaline volcanics) assemblages between 2.75 and 2.70 Ga in a region of complex plate interactions; (2) termination of volcanism by collision of a large continental mass to the south at about 2.70 Ga; (3) tectonic thickening during collision and coeval deposition of 2.70–2.68 Ma turbidite dominated assemblages; and (4) terminal subduction at 2.69–2.67 Ga generating alkalic volcanic and intrusive rocks (e.g. Lebel Stock) and alluvial–fluvial sediments spatially associated with E–W-trending crustal-scale shear zones (e.g. LCDZ).

Geology of the Kirkland Lake area

In the Kirkland Lake area (Fig. 1) the LCDZ separates a 2680–2670 Ma old sequence of alkalic metavolcanic rocks and clastic metasediments to the north, the Timiskaming Group, from a *ca* 2705 Ma old package of mafic metavolcanic rocks and turbidites to the south, the Larder Lake Group. North of the LCDZ, variably deformed rocks of the Timiskaming Group form a

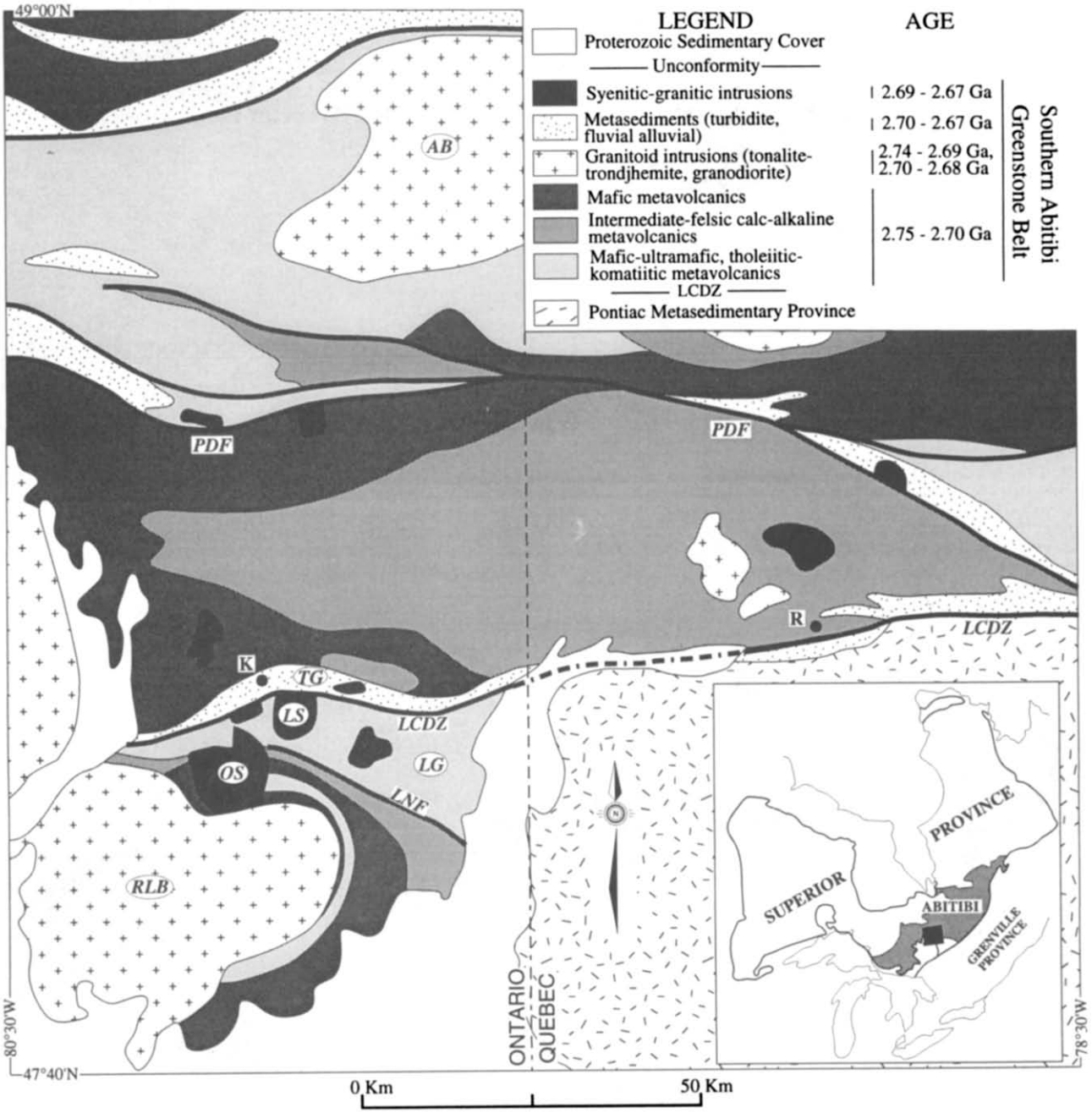

Fig. 1. Simplified geological map of the southern Abitibi Greenstone Belt (after Jackson & Fyon 1991). Insert shows location of the Abitibi Greenstone Belt (shaded) and the area covered by the main map (black box). LS, Lebel Stock; OS, Otto Stock; TG, Timiskaming Group; LG, Larder Lake Group; RLB, Round Lake batholith; AB, Abitibi batholith; LCDZ, Larder Lake–Cadillac deformation zone; PDF, Porcupine–Destor Fault; LNF, Lincoln Nipissing Fault; K, Kirkland Lake; R, Rouyn-Noranda.

steeply S-dipping homocline that rests unconformably on 2701 Ma old mafic to felsic metavolcanics. South of the LCDZ, the Larder Lake Group is faulted against a N- to NE-dipping sequence of 2747–2701 Ma old metavolcanic rocks which wrap around the 2703–2697 Ma Round Lake Batholith (Jensen 1985, Jackson & Fyon 1991).

The LCDZ in the Kirkland Lake area (Fig. 1) is a roughly E–W-trending subvertical zone of intense ductile fabric development and alteration up to 1 km wide. Recent seismic reflection surveys in the region indicate that the LCDZ dips steeply southward to a depth of at least 15 km (Jackson *et al.* 1990). Two important phases of ductile fabric development (D_1 and D_2) have been identified within the zone (Toogood & Hodgson 1986, Hodgson & Hamilton 1989, Cruden 1990a, 1991). Plausible interpretations of the fabrics and kinematic indicators associated with these deformation events include: (1) south-over-north oblique-slip shearing (D_1) followed by dextral transcurrent motion (D_2) (Hodgson & Hamilton 1989, Cruden 1990a); or (2) progressive dextral shearing with an early, strong, zone-normal flattening component (i.e. 'transpression'; Robert 1989, Robin & Cruden 1991). The relative timing of D_1 ductile fabric development in the LCDZ is constrained by the observations that D_1 structures overprint the *ca* 2680 Ma old

Lebel Stock (Fig. 2) (Cruden 1991). However, an early (pre-D_1 using the above terminology) structural history for the LCDZ as a sinistral wrench fault has been proposed by Toogood & Hodgson (1986), Ludden *et al.* (1986) and Hubert (1990) on the basis of the orientation of pre-cleavage folds, the distribution of intrusive rocks and various stratigraphic arguments. Deposition of the Timiskaming Group is also thought to have occurred within a restricted basin, structurally controlled by a pre-D_1 or 'proto-' LCDZ (Colvine *et al.* 1988, Mueller & Davidson 1991). One of the objectives of the work reported here is to establish whether there is also a

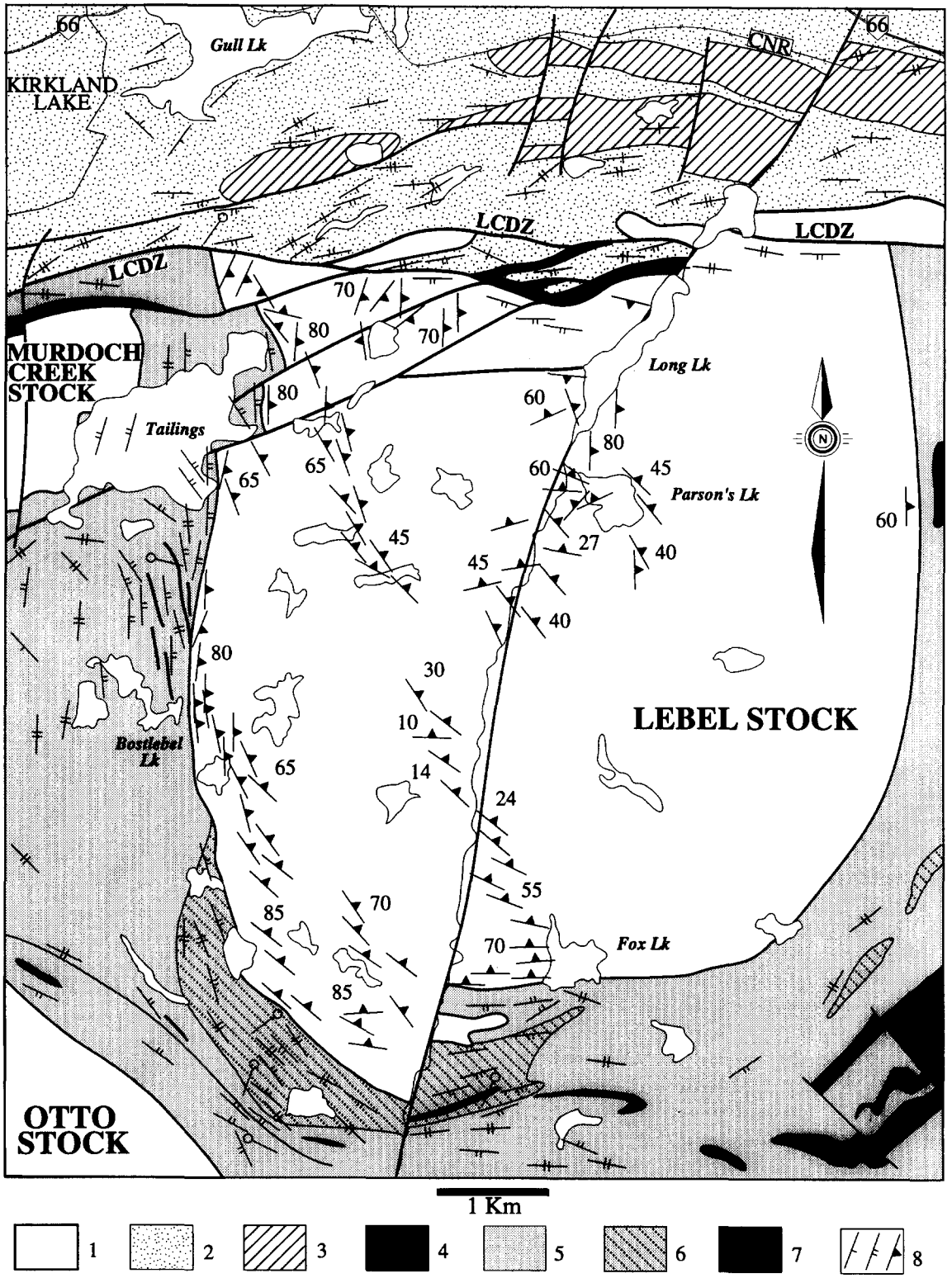

Fig. 2. Geology and structure of the Lebel Stock (partly after McLean 1956 and Lawton 1957). (1) Syenites; (2) Timiskaming Group clastic metasediments; (3) Timiskaming Group alkalic metavolcanics; (4) green carbonate schists (highly altered and deformed metabasalts and ultramafic volcanics of the Larder Lake Group); (5) Larder Lake Group (basaltic metavolcanics); (6) Larder Lake Group banded intermediate metavolcanics; (7) iron formation; (8) strike and dip of bedding/volcanic layering, foliation/cleavage in supracrustal rocks and planar magmatic fabric in syenites, respectively.

relationship between the emplacement of syenitic intrusions and the proposed proto-LCDZ.

Suites of syenitic (pyroxenite–hornblendite to alkali-feldspar syenite) and granitic (diorite to granite) intrusive rocks occur north and south of the LCDZ. Rocks in both suites occur as distinct phases in composite bodies or as discrete plutons (Levesque *et al.* 1991). The parental magmas of these intrusive rocks are considered to be mantle-derived and possibly subduction-related (Sutcliffe *et al.* 1990). The Otto stock (Fig. 1) has yielded an U–Pb zircon age of 2680 ± 1 Ma (Corfu *et al.* 1989) and a D_2 folded porphyry dyke north of the LCDZ gave an U–Pb zircon age of 2677 ± 3 Ma (Corfu *et al.* 1991). These dates plus observations that the intrusive rocks both cross-cut and occur as clasts within Timiskaming Group sediments suggest that magma emplacement and sedimentation were broadly coeval and that both occurred over a relatively short period.

THE LEBEL STOCK

The Lebel stock is located 2 km southeast of Kirkland Lake (Fig. 2). Field work and sampling was concentrated on the western two-thirds of the stock because of exposure and access. High resolution aeromagnetic data (HSK minerals, Battle Mountain Inc.) was used to constrain the poorly exposed east and northeast contacts of the pluton. Parts of the stock and its wall rocks were previously mapped by MacLean (1956) and Lawton (1957). An intrusion age of *ca* 2680 Ma is inferred for the Lebel Stock because of its petrological similarity to the adjacent, radiometrically dated Otto Stock (Corfu *et al.* 1989).

Margins and wall rock structure

South of the LCDZ the Lebel Stock intrudes mafic and intermediate metavolcanics, quartzite and iron formation of the Larder Lake Group (Lawton 1957) (Fig. 2). The contact dips steeply towards the interior of the stock. The stock is associated with a well defined, asymmetric Bouguer gravity anomaly (Gupta 1991) which indicates that the deepest part (i.e. highest anomaly values) is located in the north-central part of the intrusion, immediately south of the LCDZ. Gravity values decrease outward, toward the margin indicating that the stock is mostly a relatively thin tabular body. Intrusion of the stock appears to post-date a regional folding, foliation and faulting event which produced regional folds and faults exposed southeast and west of the stock. Contacts, bedding and pre-intrusion structures in the wall-rocks show large-scale conformity with the stock margin up to 2 km from the contact, but the stock is locally discordant at both map- and outcrop-scale (Fig. 2). This is particularly obvious along the west margin where a regional E–W, sub-vertical, weak foliation in mafic volcanics and foliation parallel iron formation beds swing towards the contact with a consistent clockwise sense (Fig. 2). Iron formation layers are eventually truncated by the stock at a low angle (5–10°) to the contact. A similar relationship is observed in an exposure of the western contact (Fig. 3) which appears to be a 'magmatic' dextral shear zone. Foliation intensity increases approaching the pluton contact and a *ca* 100 m wide layer of intensely banded rock with a strong mineral foliation and moderate down-dip lineation is developed around the western and southern margins. An approximately 1 km wide contact metamorphic aureole surrounds the stock and metamorphic grade in the country-rocks increases from greenschist to amphibolite facies approaching the margin (Lawton 1957, Jolly 1978). Structurally complex, migmatized and K-metasomatized rocks are locally developed along the southern margin.

The northern margin of the stock is truncated by the LCDZ. Here a 5–20 m wide band of syenite gneiss is faulted against strongly deformed Timiskaming Group meta-sediments (sericite schists and strained meta-conglomerates) and slivers of highly altered and deformed ultramafic and mafic metavolcanic rocks (green carbonate and amphibolitic schists) of the Larder Lake Group. Slices of deformed and altered syenite are tectonically interleaved with metasediments and metavolcanics within a 500 m wide zone north of the stock. The relative age of the syenite intrusion and Timiskaming Group sediments is not locally constrained. MacLean (1956) reports cross-cutting relationships between syenite dykes and meta-sediments north of the Lebel Stock, indicating that the stock post-dates Timiskaming Group

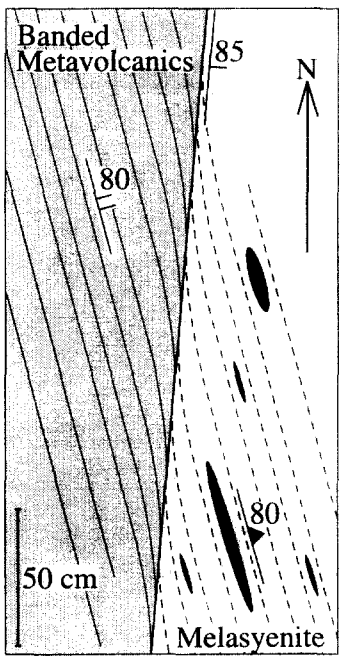

Fig. 3. Sketch of a horizontal surface of an exposed contact of the Lebel Stock, located *ca* 200 m southeast of the southeastern corner of the large tailings pond shown in Fig. 2. Solid thin lines = banding in mafic metavolcanics; dotted lines = trace of planar preferred mineral and mafic microgranular enclave (black ellipses) fabric in syenite. Note how emplacement-related fabrics in the wall rock and the pluton rotate into parallelism with the contact which is oblique to the main trend on either side, indicating southward flow of magma during intrusion.

deposition but pre-dates LCDZ ductile fabric development. The relatively young, NNE-trending Long Lake Fault (LLF) cuts through the stock and offsets both its southern and northern margins and the trace of the LCDZ (Fig. 2).

Internal structure and petrology

The stock shows a weak, transitional, normal compositional zonation. A 50–100 m wide marginal zone of medium- to coarse-grained alkali-feldspar melasyenite grades into coarse-grained alkali-feldspar syenite which occupies most of the central regions of the stock. Small, sporadic occurrences of hornblendite and meladiorite occur along the margins and as rare elliptical enclaves within the stock. Magma mingling relationships are observed between these mafic phases and the alkali-feldspar syenite indicating coeval intrusion. Rowins *et al.* (1991) interpret similar petrological variations in the adjacent Murdoch Creek Stock (Fig. 2) to indicate that the pluton intruded as a single pulse of previously evolved magma. Poikilitic clinopyroxene (diopsidic; biotite and magnetite inclusions), biotite, magnetite, minor apatite and sphene make up about 35 vol.% of the marginal melasyenite with tabular, elongate perthitic orthoclase as the dominant felsic constituent. In the alkali-feldspar syenite mafic minerals (pyroxene ≫ biotite) make up 10–20 vol.% of the rock and magnetite, sphene, apatite and zircon are accessory phases. Pyroxene is often partly replaced by pale green actinolite at its margins. In both rocks magnetite occurs mainly as interstitial polycrystalline aggregates in clots together with the mafic phases. It is often found to lie along grain boundaries and less frequently as anhedral inclusions in clinopyroxene and cleavage parallel inclusions in biotite. Following Rowins *et al.*'s (1991) study of magmatic oxidation in the Murdoch Creek Stock, magnetite is considered to be primary in origin, except where syenites are affected by local deformation and alteration related to the LCDZ and LLF.

Most outcrops in the stock show a planar preferred orientation of tabular K-feldspar, elongate clinopyroxene grains and interstitial mafic mineral aggregates (Fig. 4a). This fabric is most intense in the marginal zones of the stock and shows an apparent inward decrease as grain size increases. No linear fabric could be discerned in the field. The planar fabric is generally parallel to the stock margins (Fig. 2) and at the current erosion level defines a dish- or spoon-like structure in accordance with the regional gravity data (Gupta 1991). The fabric dips steeply toward the centre of the intrusion at the contact, and dips gradually decrease to generally shallow northward inclinations in the center. The fabric pattern in the western part of the stock mirrors the foliation swing observed in the wall-rocks; the NE-striking fabric in the interior and at the southern margin swings in a consistent clockwise sense into parallelism with the N-trending western contact. The N-striking fabric in the northeastern area of the stock is clearly truncated by the LCDZ (Fig. 2).

The internal fabric of the stock is interpreted to have been acquired as a result of magmatic flow (e.g. Paterson *et al.* 1989, Cruden 1990b) during emplacement based on the following criteria: (1) neither primary igneous minerals (K-feldspar, pyroxene, biotite) nor interstitial matrix materials show any evidence of plastic deformation or recrystallization (Fig. 4b); (2) aligned K-feldspars show zoning and Carlsbad twinning, and clinopyroxenes commonly exhibit zoning, indicating crystallization from a magma. Some samples show evidence that flow may have continued into the submagmatic stage, as indicated by melt filled fractures in K-feldspar (Fig. 4c) (e.g. Hibbard 1986, Bouchez *et al.* 1992) and localized strain features (e.g. bending of biotite grains) at grain–grain contacts. Evidence for grain interaction during emplacement of the stock is not surprising, given the low proportion of late crystallizing, interstitial material remaining in the rock.

Apparently unstrained samples taken from the northern part of the stock, up to 200 m south of the LCDZ, contain E–W-trending, spaced, hairline fractures at a high angle to the preferred orientation of K-feldspars and mafic minerals (Fig. 4d). They also show extensive carbonate alteration and precipitation of secondary magnetite along the fractures. A second group of samples collected from outcrops close to the southern end of Long Lake (Fig. 2) show a weak to moderate solid-state foliation and alteration which are interpreted to be related to the LLF. These local, low-strain solid-state deformation features can strongly modify the magnetic fabric of the rock as discussed below.

MAGNETIC FABRIC OF THE LEBEL STOCK

Magnetic susceptibility, κ, is a symmetrical second-rank tensor coefficient relating the two vector properties, induced magnetic moment J, and the inducing magnetic field H (Nye 1985). The anisotropy of magnetic susceptibility is conveniently expressed as a magnitude ellipsoid (Hrouda 1982, Nye 1985) with principal axes, $k_{max} > k_{int} > k_{min}$. The average or bulk susceptibility is given as $K = (k_{max} + k_{int} + k_{min})/3$. Instrumentation for AMS determination (e.g. Collinson 1983), its application in geology and geophysics (e.g. Hrouda 1982), statistical processing (e.g. Jelinek 1978) and presentation of data (e.g. Borradaile 1988, Ellwood *et al.* 1988) are well reviewed in the literature. Low field magnetic susceptibility in rocks is thought to be due to additive contributions from diamagnetic, paramagnetic (the 'rock matrix' of Rochette 1987) and ferrimagnetic minerals (Henry 1983, Borradaile 1988). Diamagnetic susceptibility is usually very low ($\approx -14 \times 10^{-6}$ SI) and calcite is the only diamagnetic mineral with a significant degree of anisotropy ($P = k_{max}/k_{min}$) of 1.13 (Rochette 1987). In rocks with $K \ll 10^{-3}$ SI ($< \approx 1$ wt % magnetite) or $P \ll 1.35$ the paramagnetic mineral contribution to the AMS is thought to become significant (Rochette 1987, Borradaile 1988).

The origin of low field magnetic anisotropy in rocks is considered to be mainly due to: (1) shape alignment of ferrimagnetic grains; and (2) lattice alignment of crystals with marked magnetocrystalline anisotropy (Stacey 1960, Uyeda *et al.* 1963). Anisotropic distribution of magnetite may also contribute to AMS in some rocks (Stacey 1960, Hargraves *et al.* 1991). AMS studies of granitoids find a strong correlation between the rock fabric (foliation and lineation when visible) and the magnetic foliation ($F = k_{int}/k_{min}$) and lineation ($L = k_{max}/k_{int}$) (e.g. King 1966, Guillet *et al.* 1983, Rathore & Kafafy 1986, Bouchez *et al.* 1990). Even in plutons with extremely weak grain orientations, the AMS fabric commonly shows a consistent pattern throughout the intrusion (e.g. Ellwood & Whitney 1980, Gleizes & Bouchez 1991). Cogné & Perroud (1988) found a positive correlation between the shape and magnitude of the susceptibility and magmatic (?) strain ellipsoids (determined from deformed enclaves) in the Flammanville granite. Launeau (1990) reports a good agreement between AMS parameters and mineral anisotropy in a combined AMS–image analysis study of the Mont-Louis-Andorra pluton, in which the magnetic fabric is defined entirely by paramagnetic phases (biotite and amphibole). It is, however, not yet well established how magnetic fabric parameters relate to the bulk anisotropy of granitic rocks in which the AMS is defined by ferrimagnetic phases. This is because the magnetic fabric is no longer directly related to the preferred orientation of paramagnetic minerals, but to that of low volume percent magnetite grains.

Sampling and AMS determination

Oriented block samples were collected from 23 stations within the Lebel Stock (Fig. 5). From these a total of 132 cylinders, 2.2 cm (length) × 2.54 cm (diameter), were prepared for AMS measurement. Sampling was restricted to the main phase alkali-feldspar melasyenites and alkali-feldspar syenites. The eight samples collected from sites weakly to moderately affected by deformation and alteration associated with the LCDZ and LLF are indicated in Fig. 5. All other samples are fresh and show no signs of solid-state strain or alteration.

Magnetic susceptibility and its anisotropy was determined using a Sapphire Instruments SI-2 induction coil instrument. The absolute accuracy of susceptibility measurements on our instrument is estimated to be better than 98% for samples with $K > 3.77 \times 10^{-4}$ SI. Statistical averaging of AMS data from individual sites was carried out using the program AMSSTAT which calculates variances and standard deviations of principal axis lengths and directions using the matrix averaging routines recommended by Hext (1963) and Jelinek (1978).

Results

AMS data are presented in Table 1 in terms of site means and variability. Susceptibilities (means and standard deviations) and their azimuth and inclination were calculated using unweighted data. In addition to P, L and F (means and standard deviations) three other parameters are also included: $Flinn = (L - 1)/(F - 1)$, $T = [2(\ln k_{int} - \ln k_{min})/(\ln k_{max} - \ln k_{min})] - 1$, and $P' = \exp[2(a_1^2 + a_2^2 + a_3^2]^{1/2}$, where $a_1 = \ln(k_{max}/kb)$, etc., and $kb = (k_{max} \cdot k_{int} \cdot k_{min})1/3$, after Flinn (1962) and Jelinek (1981), respectively. *Flinn* and T are measures of the shape of the susceptibility ellipsoid, and P' expresses the degree of anisotropy as discussed by Borradaile (1988).

Susceptibility values. All rocks measured have high K values averaging 3.7×10^{-2} SI. This is well above the 10^{-3} SI value indicative of a paramagnetic contribution (Rochette 1987, Borradaile 1988). Both the high bulk susceptibilities and observations of high (≥1 vol.%) volume percentages of magnetite in thin sections indicate that the AMS in these syenites is due to magnetite. Bulk susceptibility shows no strong spatial variation within the pluton, although marginal melasyenites tend to show values *ca* 10% higher than the average. No correlation exists between bulk susceptibility and anisotropy degree, indicating that AMS fabric strength is independent of composition in these rocks (e.g. Borradaile 1987).

Directional data. AMS fabric data from 15 representative sites throughout the Lebel Stock are shown in Fig. 6. Principal axes generally fall within a 10–20° elliptical cone about the matrix averages for any one site. Samples showing very tight k_{max} clusters and a spread of k_{min} directions tend to be characterized by prolate magnetic fabrics (see below) whereas those showing the widest dispersion of k_{max} axes have an oblate AMS ellipsoid. For most sites the magnetic foliation (k_{max}/k_{int} plane) agrees with the planar fabric measured in the field to within 15° (Fig. 7a). Significant departures from the mesoscopic fabric are observed in samples taken close to the LCDZ and LLF. For example, sample AC90 032 (Fig. 6) shows a moderate grain orientation fabric dipping steeply eastward, whereas its magnetic foliation is inclined steeply to the north. Although not obvious in

Fig. 4. (a) General appearance of planar preferred orientation fabric on polished slab of marginal K-feldspar melasyenite. Scale bar = 1 cm. (b) Thin section of K-feldspar melasyenite with strong preferred mineral orientation fabric defined by K-feldspar laths, clinopyroxene laths and mafic aggregates (clinopyroxene, biotite, sphene, magnetite). Opaque phase is magnetite, which is usually anisotropic and aligned parallel to the bulk fabric. Plane polarized light. Width of photograph = 12 mm. (c) Thin section of K-feldspar syenite showing brittle fracture of a large twinned K-feldspar grain, filled with fine-grained late-crystallizing material. Note minimal offset of K-feldspar grain and confinement of fracture to a single grain (viz. Bouchez *et al.* 1992). Cross polars. Width of photograph = 12 mm. (d) Thin section of K-feldspar syenite sample collected *ca* 100 m south of the LCDZ. East–west-trending, magnetite filled, hairline fractures are orthogonal to a N–S-trending preferred mineral orientation fabric. Note alteration (chloritization and carbonatization) of mafic mineral aggregates. Plane polarized light. Width of photograph = 12 mm.

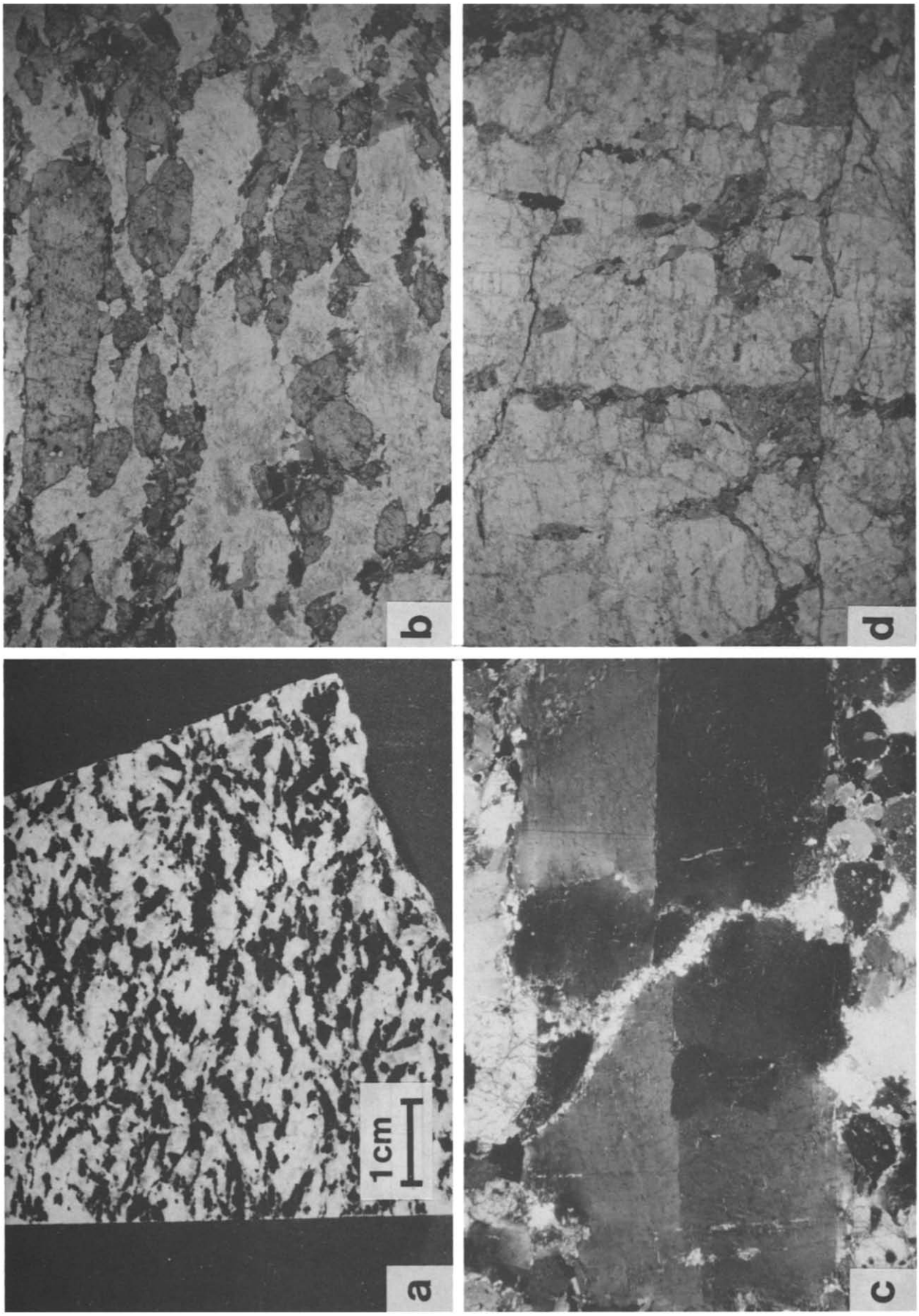

Fig. 4.

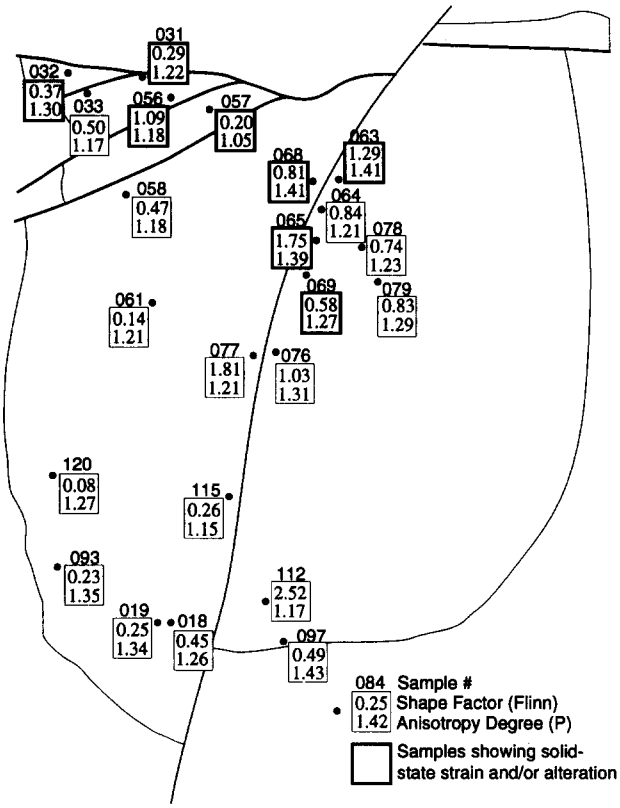

Fig. 5. Sample locations for AMS determination. Boxes contain AMS ellipsoid shape and intensity parameters for each analysis (see text). Samples showing solid-state strain and/or alteration features are indicated by thick rimmed boxes.

outcrop, this sample and others from close to the LCDZ have E–W-trending hairline fractures containing secondary magnetite in thin section (e.g. Fig. 4d). Hence, the AMS fabric in these rocks is extremely sensitive to later solid-state strains and alteration. The following discussion of AMS directional data will therefore concentrate on results from samples unaffected by post-magmatic LCDZ- and LLF-related strains.

The magnetic foliation pattern of the stock matches that shown by the magmatic foliation measured in the field (Fig. 7a). AMS fabrics of Lebel Stock syenites also contain a well-defined magnetic lineation (k_{max}, Fig. 7b). With the exception of sites along the stock's southern margin (e.g. samples AC90 018, 019, 093, 097, 112, 120; Figs. 5 and 6) magnetic lineations show a strong N–S-trend and mostly plunge shallowly to moderately northwards (Fig. 7b). Lineations in samples along the southern margin consistently plunge moderately to the east and southeast (Fig. 7b).

AMS parameter variation. Figure 8 summarizes the range of AMS ellipsoid shapes and intensities within the Lebel Stock. The majority of magnetic fabric ellipsoids fall within the general flattening field on a Flinn diagram (Fig. 8a). Jelenek's T vs P' plot (Fig. 8b) demonstrates that there is no correlation between susceptibility ellipsoid shape and the degree of anisotropy. A weak spatial variation of AMS parameters is observed (Fig. 5). Samples from the north central part of the stock around Parson's Lake (Fig. 2) have plane to prolate type AMS ellipsoids with $Flinn \approx 0.7$–1.8, whereas those from outside this region show oblate fabrics ($Flinn < 0.7$) with only two exceptions. Half of the six samples with prolate ($Flinn > 1.0$) magnetic fabrics have been affected by either solid-state strains (e.g. AC90 063 and 065) or LCDZ-related alteration (e.g. AC90 056). Two others (AC90 076 and 077) collected from close to the LLF show no obvious signs of a solid-state overprint but are weakly altered. Plane to prolate AMS ellipsoids in these rocks may therefore be indicative of solid-state overprinting and/or secondary magnetite precipitation dur-

Table 1. Anisotropy of magnetic susceptibility, means and parameters

Sample				Kmax				Kmin												
No.	N	K (SI)	±	Az.	Inc.	K_1	±	Az.	Inc.	K_3	±	P	±	L	±	F	±	$Flinn$	T	P'
AC90.018	6	0.058	0.012	103	45	0.063	0.007	197	4	0.05	0.001	1.26	0.16	1.08	0.13	1.17	0.03	0.45	0.36	1.22
AC90.019	6	0.036	0.007	102	79	0.041	0.001	253	10	0.03	0.001	1.34	0.06	1.07	0.05	1.26	0.05	0.25	0.57	1.28
AC90.031	4	0.043	0.007	167	23	0.046	0.001	343	67	0.038	0.001	1.22	0.08	1.05	0.07	1.16	0.09	0.29	0.53	1.18
AC90.032	2	0.039	0.002	287	24	0.044	0.002	189	16	0.034	0.002	1.30	0.17	1.08	0.09	1.21	0.13	0.37	0.44	1.25
AC90.033	3	0.053	0.006	195	2	0.057	0.002	287	31	0.048	0.002	1.17	0.09	1.06	0.06	1.11	0.08	0.50	0.32	1.14
AC90.056	9	0.044	0.014	25	41	0.048	0.001	238	44	0.041	0.002	1.18	0.08	1.09	0.05	1.08	0.07	1.09	−0.04	1.15
AC90.057	6	0.06	0.018	192	19	0.006	0.001	339	68	0.006	0.001	1.05	0.28	1.01	0.26	1.04	0.28	0.20	0.66	1.04
AC90.058	9	0.035	0.01	330	6	0.037	0.001	234	54	0.032	0.001	1.18	0.09	1.06	0.08	1.12	0.09	0.47	0.35	1.15
AC90.061	6	0.033	0.005	346	8	0.035	0.001	243	55	0.029	0.001	1.21	0.11	1.02	0.08	1.18	0.11	0.14	0.75	1.18
AC90.063	6	0.038	0.007	356	42	0.045	0.001	234	31	0.032	0.0004	1.41	0.03	1.21	0.04	1.16	0.04	1.29	−0.12	1.35
AC90.064	9	0.035	0.01	348	18	0.039	0.001	232	54	0.0321	0.001	1.21	0.08	1.09	0.06	1.11	0.07	0.84	0.08	1.18
AC90.065	11	0.039	0.015	5	12	0.046	0.001	116	58	0.033	0.001	1.39	0.08	1.23	0.05	1.13	0.06	1.75	−0.25	1.34
AC90.068	4	0.031	0.003	48	48	0.036	0.001	262	37	0.025	0.001	1.41	0.13	1.17	0.09	1.21	0.13	0.81	0.09	1.35
AC90.069	6	0.014	0.001	356	17	0.016	0.002	225	65	0.013	0.002	1.27	0.49	1.09	0.37	1.16	0.45	0.58	0.26	1.22
AC90.076	8	0.042	0.012	195	6	0.048	0.002	293	50	0.037	0.002	1.31	0.15	1.14	0.10	1.14	0.11	1.03	−0.01	1.26
AC90.077	3	0.03	0.002	137	4	0.033	0.001	232	53	0.028	0.001	1.21	0.11	1.13	0.11	1.07	0.12	1.81	−0.28	1.19
AC90.078	3	0.03	0.002	8	62	0.033	0.001	212	26	0.027	0.001	1.23	0.12	1.09	0.10	1.13	0.13	0.74	0.14	1.19
AC90.079	6	0.029	0.004	161	2	0.033	0.001	254	52	0.025	0.001	1.29	0.13	1.12	0.11	1.15	0.12	0.83	0.09	1.24
AC90.093	6	0.031	0.005	108	55	0.034	0.001	224	17	0.026	0.001	1.35	0.08	1.06	0.05	1.27	0.07	0.23	0.59	1.29
AC90.097	10	0.06	0.033	118	35	0.07	0.001	215	10	0.049	0.001	1.43	0.05	1.13	0.04	1.27	0.07	0.49	0.32	1.35
AC90.112	6	0.051	0.013	87	39	0.055	0.001	225	42	0.047	0.0004	1.17	0.02	1.12	0.03	1.05	0.02	2.52	−0.42	1.16
AC90.115	5	0.027	0.003	203	13	0.029	0.001	343	73	0.025	0.001	1.15	0.10	1.03	0.09	1.12	0.10	0.26	0.57	1.13
AC90.120	4	0.04	0.005	348	3	0.043	0.002	257	19	0.034	0.002	1.27	0.14	1.02	0.09	1.24	0.13	0.08	0.84	1.23

Az., Inc. = mean azimuth and inclination of principal axis. K_1, K_3 = magnitudes of maximum and minimum susceptibilities (SI units). See text for definition of AMS parameters.

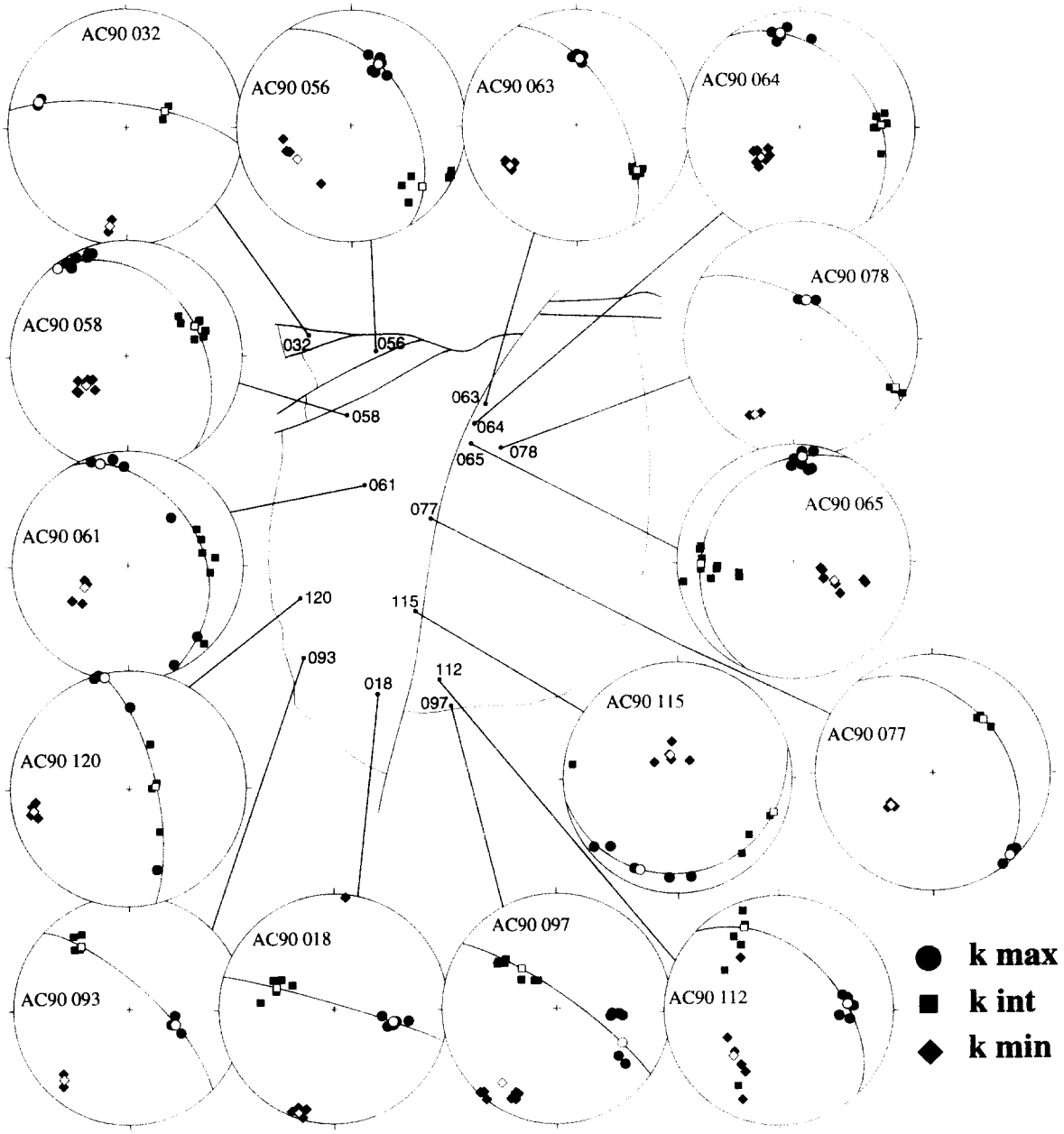

Fig. 6. Equal-area, lower-hemisphere projections of AMS principal axis directions for 15 representative examples of the 23 sites analyzed. Open symbols are mean directions, great circles are best-fit magnetic foliation planes.

ing alteration. Anisotropy degree (P) values show a wide scatter throughout the pluton, although sites within the north-central region and along the south and southwest margin have higher values ($P > 1.25$) than the intervening region. With the exception of samples affected by LCDZ- and LLF-related strains and alteration, the Lebel Stock is therefore characterized by oblate type fabrics which increase in intensity approaching the southern margin.

Significance of the AMS data

The high bulk susceptibility and relatively high volume percent of magnetite in the Lebel Stock syenites indicate a ferrimagnetic origin for the AMS. In undeformed and unaltered samples the bulk of magnetite grains are found as generally elongate polycrystalline aggregates which occur together with pyroxene, biotite, sphene and apatite as interstitial mafic clots aligned parallel to the preferred orientation of larger K-feldspar grains (Fig. 4b). Although this indicates qualitatively that their AMS probably corresponds to the magmatic fabric, we have further investigated the cause of AMS in these rocks by using quantitative image analysis techniques. A detailed account of this work will be presented elsewhere and only results pertinent to establishing the relationship between the magnetic and magmatic fabrics in the Lebel Stock are discussed here.

The shape preferred orientations (SPO) of populations of K-feldspar, pyroxene and biotite+magnetite grains were measured on digital images of large thin sections cut parallel to the principal planes of the AMS ellipsoids of samples AC90 018, 056, 061, 065, 093 and 097 using the methods described by Launeau (1990) and

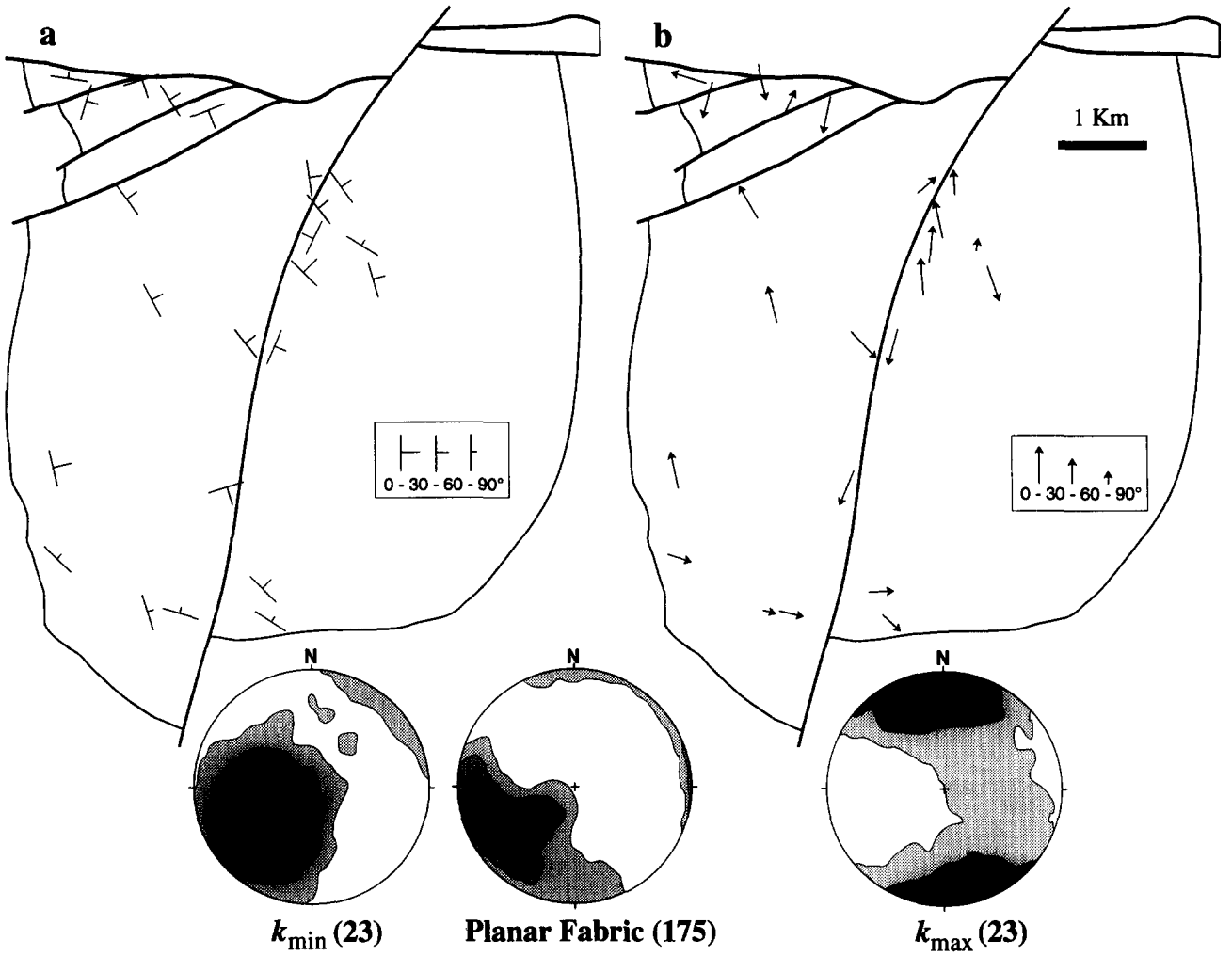

Fig. 7. Magnetic foliation (a) and lineation (b) maps for the Lebel Stock. Kamb contoured equal-area lower-hemisphere projections of k_{max} (= magnetic lineation, contour interval 2σ), poles to planar magmatic fabric measured in the field (contour interval 3σ) and k_{min} (= pole to magnetic foliation, contour interval 2σ) are shown below the maps.

Launeau & Bouchez (1992). The SPO of each mineral population was measured globally using the intercept technique (Launeau *et al.* 1990). Biotite and magnetite were treated together in the SPO analysis because of technical difficulties in separating these minerals in the digital images. Fabric intensity is expressed as the aspect ratio ($SR_{mineral}$) of the fabric ellipse and fabric orientation is given by $\alpha°$, the angle between the long axis of the fabric ellipse and the trace of the maximum AMS direction on the plane of analysis. Figure 9(a) shows that $\alpha°$ for each mineral SPO is always within 25° of, and symmetrically distributed about the maximum susceptibility direction, with the exception of principal planes with a $SR_{mineral} < 1.10$. This indicates that principal magnetic fabric directions are parallel to the magmatic fabric axes in the Lebel Stock syenites. The poor correlation between magnetic and mineral fabric directions on surfaces with $SR_{mineral} < 1.10$ is due to the difficulty in determining the principal SPO direction when the fabric intensity is extremely low, as is the case on the k_{max}/k_{int} planes of samples with strongly oblate magnetic fabrics.

Mineral fabric and magnetic fabric intensities are strongly correlated. This is illustrated by the comparison of $SR_{K\text{-feldspar}}$ and SR_{AMS} (the aspect ratio of principal sectional susceptibility ellipses) in Fig. 9(b). This almost one-to-one relationship is expressed by the least-squares regression line $SR_{K\text{-feldspar}} = 0.98\ SR_{AMS} + 0.07$, with coefficient of determination $r^2 = 0.63$. Similarly, results for the two other mineral populations are $SR_{pyroxene} = 0.80\ SR_{AMS} + 0.26$ ($r^2 = 0.74$) and $SR_{biotite+magnetite} = 0.56\ SR_{AMS} + 0.46$ ($r^2 = 0.61$). The relatively poor correlation between the AMS and the biotite+magnetite fabrics is thought to be due to the small number of these grains occurring in each thin section (about 3%), and the grouping together of two different minerals, rather than to any real difference between them. Since K-feldspar makes up between 75 and 90% of these rocks it can be concluded that AMS is a good measure of the bulk SPO intensities and directions in the Lebel Stock.

The magnetite anisotropy degree values of the syenites are very high, as is the qualitative fabric strength observed in outcrop and hand sample (e.g. Fig. 4a). Hrouda (1982) considers values of $P' \geq 1.2$ in plutonic rocks to be due to either mimetic (i.e. secondary) magnetic or to later solid-state strain. This is because the grain orientation mechanism of the ferrimagnetic and matrix minerals assumed to operate in flowing magma (i.e. 'Marchian' rotation; King 1966, Owens 1974) is

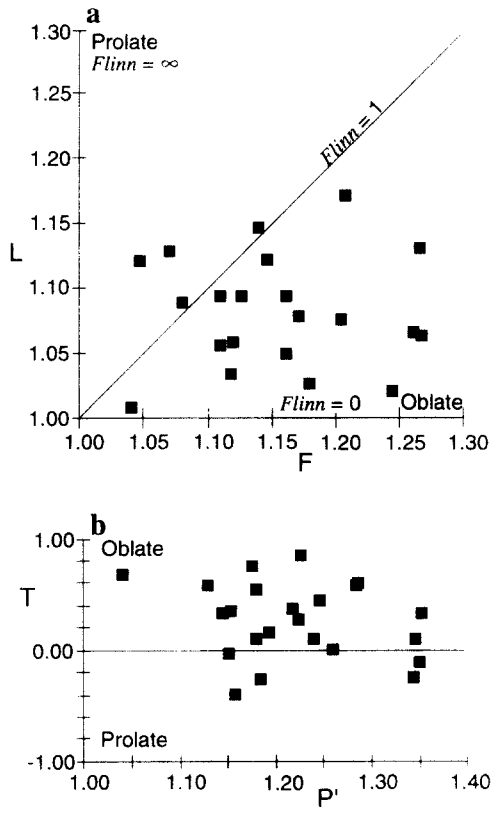

Fig. 8. AMS ellipsoid shape and intensity parameters: (a) Flinn diagram, (b) Jelinek's T vs P' plot. See text and Table 1 for definitions of parameters.

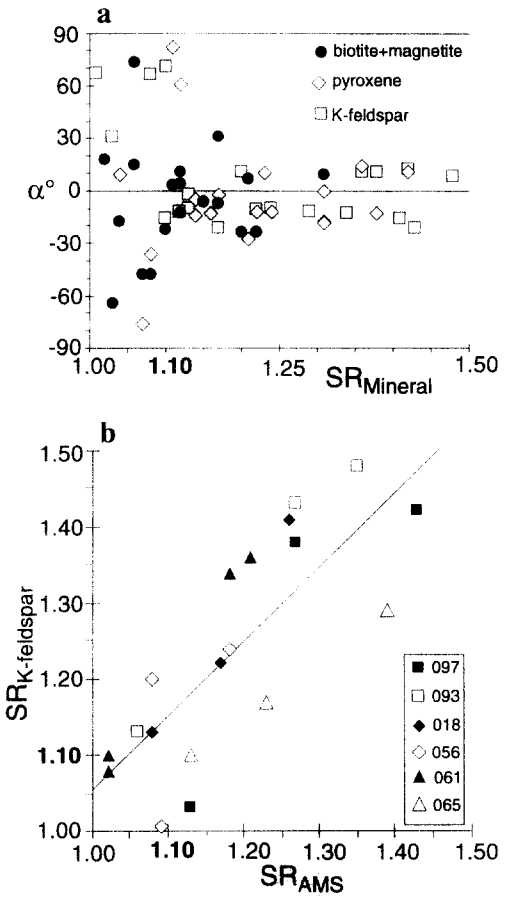

Fig. 9. Results of the image analysis study of six representative samples of Lebel Stock syenite. (a) Shows that the angle ($\alpha°$) between the mineral fabric axes and principal susceptibility directions (measured on thin sections cut parallel to the three principal planes of the AMS ellipsoids of the samples) is <25° except for surfaces on which the mineral fabric intensity is extremely weak ($SR_{mineral} < 1.10$). (b) Correlation between the intensity of the K-feldspar fabric ($SR_{K\text{-}feldspar}$) and the principal AMS sectional ellipses (SR_{AMS}) for the samples analyzed. Slope of the least-squares regression line is 0.98. See text for further details.

relatively ineffective. However, the occurrence of free grain rotation during the final stages of emplacement of the Lebel Stock magma cannot be assumed, given the low proportion of interstitial material preserved in the rock and the microstructural evidence for grain–grain interaction (i.e. sub-magmatic flow features). The very strong SPOs displayed by the Lebel Stock syenites are similar to those shown by tabular feldspars in some gabbros (e.g. Oman Ophiolite; Nicolas 1992). Analogue modelling reported by Nicolas *et al.* (1993) indicates that this type of SPO can form in magmas with <20% melt during combined progressive simple and pure shear flow. Furthermore, experimental work by Ildefonse & Fernandez (1988) and Ildefonse *et al.* (1992) on the behavior of high particle concentrations during progressive simple shear has shown that fabrics lie closer to the flow plane and have a greater ability to record the finite stretch direction than those acquired when particles do not interact. In progressive pure shear the long axes of particles rotate toward the maximum principal flow direction regardless of particle concentration (Fernandez 1988, Ildefonse *et al.* 1992). Given the correlation observed above between the magnetic fabric and magmatic mineral fabric axes it is therefore reasonable to conclude that the magnetic foliations and lineations measured in the Lebel Stock syenites are parallel to the flow planes and directions of the magma during emplacement. The oblate character and generally high intensities of the AMS ellipsoids in samples unaffected by later solid-state strain and alteration suggest that the fabric was acquired by combined progressive pure and simple shear flow of a crystal laden magma (viz. Nicolas *et al.* 1993).

EMPLACEMENT OF THE LEBEL STOCK

At the current level of exposure the Lebel Stock resembles a diapiric intrusion: wall-rock structure and internal fabric are grossly concordant with the sub-circular margin in plan view. However, the inwardly shallowing magnetic and magmatic foliations (Figs. 2 and 7a), the predominantly northward trend of the magnetic lineation (Fig. 7b) and the inferred tabular geometry of the stock are not predicted by diapir models (e.g. Dixon 1975, Cruden 1990b). From the above discussion on the significance of AMS, the magnetic lineation is predicted to trend parallel to the magma flow direction, hence the bulk of the Lebel Stock magma must have been flowing north or south during emplacement. The pronounced structural asymmetry observed along the western margin (Fig. 2) strongly suggests that this flow was directed southward. The most likely source

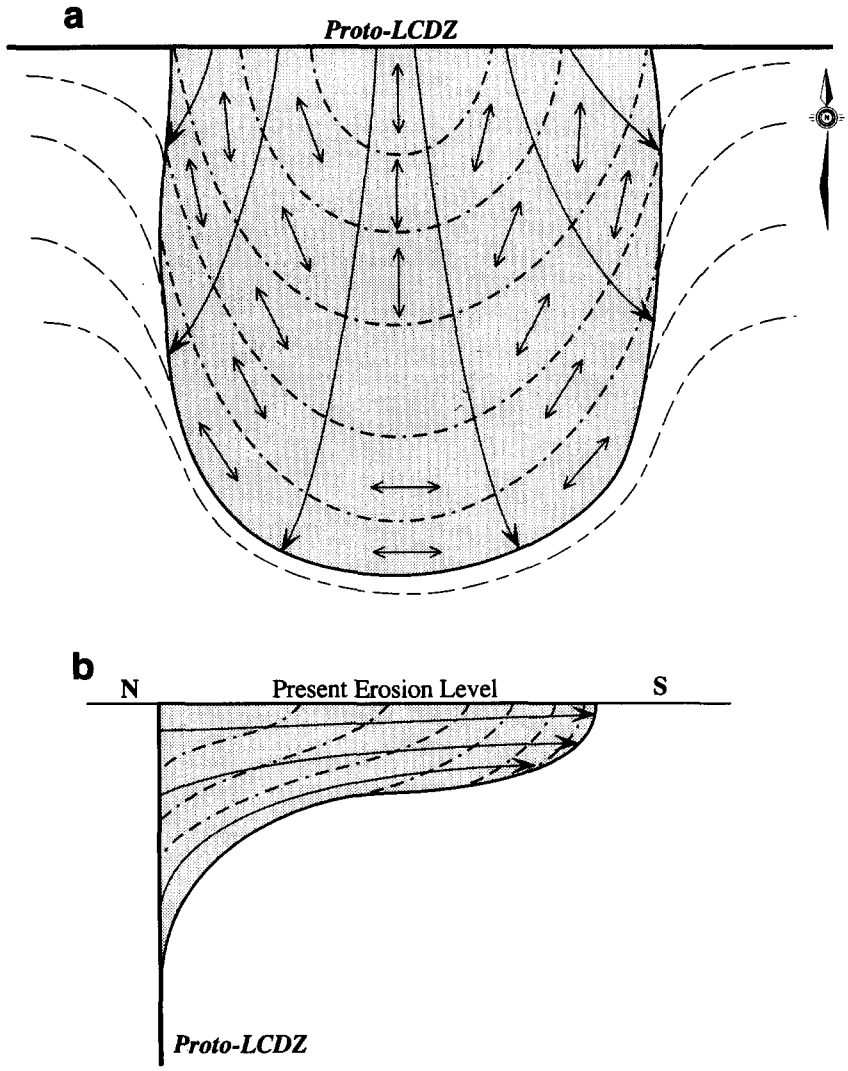

Fig. 10. Conceptual model for the emplacement of the Lebel Stock. (a) Plan view of current erosion level, (b) N–S cross-section. Solid lines with arrows are particle movement paths, dotted lines are passive marker horizons, double-headed arrows are maximum stretching directions. Note that the intersecting passive marker lines and particle paths define a crude strain grid.

for the magma is the proto-LCDZ (see Geological Setting).

A conceptual model for the emplacement of the Lebel Stock is outlined in Fig. 10. Dyke-like ascent of syenitic magma follows the proto-LCDZ until it is arrested by either reaching a level of neutral buoyancy (e.g. Lister & Kerr 1991) or by one of several alternative magma-stopping mechanisms (e.g. rheological/stress barriers, intersection with a freely slipping fracture, etc.) as discussed by Clemens & Mawer (1992). The magma begins to pond and spreads preferentially southward as a relatively thin, outwardly shallowing sheet (Fig. 10b). Southward migration of the magma sheet is accommodated by ductile deformation of the wall-rocks. Flow within the spreading intrusion is analogous to that within the toe of a flowing Piedmont glacier: instantaneous stretching directions point to the fluid source (i.e. proto-LCDZ), except at the snout of the intrusion where they are parallel to the margin due to convergence of magma as it approaches a rigid interface (Fig. 10a). The flow mechanism within the migrating sheet is expected to be by combined progressive pure and simple shear. The former resulting from convergence of magma toward the southern margin (Fig. 10a) and the latter from the vertical velocity gradient within the sheet (Fig. 10b). Southward migration eventually stops and the final magmatic and magnetic fabric of the pluton is acquired when the crystal content of the magma exceeds a critical percentage, after which it essentially behaves as a solid. This percentage is thought to be 30–40% (Arzi 1977, Van der Molen & Paterson 1979) if no shear is applied, but as shown by Nicolas *et al.* (1993) may be as low as 10% if there is a simple shear component in the flow as proposed here.

While the above scenario is somewhat simplistic it predicts a number of the structural features shown by the Lebel Stock: (1) the pronounced asymmetry of the fabrics on either side of its western boundary; (2) the inwardly shallowing, generally N-dipping magmatic foliation; (3) the change from N–S-trending, subhorizontal magnetic lineations throughout most of the pluton to E–W-trending lineations near the southern margin; and (4) AMS ellipsoids characteristic of general flattening strains with greatest intensity at the southern

margin. Furthermore, lateral spreading of a tabular pluton is a far more effective mechanism, in terms of how much wall-rock must be deformed, for space creation than diapiric intrusion or expansion of a cylindrical or spherical body (Paterson & Fowler 1993). Given that diapiric ascent is only likely to be an effective magma transport mechanism in the ductile lower- to mid-crust (Mahon *et al.* 1988), and that the 2680 Ma syenitic rocks in the Kirkland Lake area are thought to be mantle derived (Sutcliffe *et al.* 1990), then fracture propagation (Lister & Kerr 1991, Clemens & Mawer 1992) is an attractive mechanism to transport the Lebel Stock magma the required 30–40 km through the Archean crust. The proto-LCDZ acted as a convenient locus for dyke ascent.

Post-emplacement strains associated with the main (D_1) ductile fabric forming event within the LCDZ have strongly modified both the structure of the northern margin of the stock as well as AMS fabrics immediately to the south. An understanding of the relationships between the Lebel Stock and the pre- and post-emplacement structural history of the LCDZ has important implications for the late Archean tectonic history of the southern Abitibi Greenstone Belt (Cruden 1991). Ductile fabric development and Au-deposition associated with displacements on the LCDZ is constrained to be younger than about 2680 Ma (i.e. inferred emplacement age of Lebel Stock). However, the internal structure of the stock and the emplacement mechanism that it suggests provide further evidence for the existence of an important older, pre-2680 Ma, regional structure.

CONCLUSIONS

Field and microstructural examination of the Lebel Stock syenites reveals that most locations within the stock possess a strong preferred mineral orientation fabric which was acquired by magmatic to sub-magmatic flow. Well defined AMS fabrics are controlled primarily by magnetite grains and principal susceptibility axes are considered to be parallel to the magmatic fabric axes, except in rocks which have a solid-state deformation overprint. The overall oblate character of the AMS ellipsoid, the magnetic foliation and lineation pattern and the structure of the stocks's western margin have been used to suggest an emplacement mechanism. Southward migration of a relatively thin sheet of magma from an E–W-trending linear source, corresponding to the location of a major regional fault (proto-LCDZ) best explains the data.

Acknowledgements—Mike Peshko and Claudia Riveros are thanked for assistance in the field and the laboratory. Wayne Benham and Keith Barrons (Battle Mountain, Canada Inc.) and Bill McGuinty (Queenston Mining Inc.) are thanked for access to properties and invaluable information. The comments of W. M. Schwerdtner, J. Stamatakos and an anonymous reviewer helped to improve the paper substantially. This work was funded by Natural Sciences and Engineering Research Council of Canada Operating and Lithoprobe Grants to ARC and an NSERC International Fellowship to P. Launeau. Lithoprobe Contribution 450.

REFERENCES

Arzi, A. A. 1978. Critical phenomena in the rheology of partially melted rocks. *Tectonophysics* **44**, 173–184.

Borradaile, G. J. 1987. Anistropy of magnetic susceptibility: rock composition versus strain. *Tectonophysics* **138**, 327–329.

Borradaile, G. J. 1988. Magnetic susceptibility, petrofabrics and strain. *Tectonophysics* **156**, 1–20.

Bouchez, J.-P., Delas, C., Gleizes, G., Nédélec, A. & Cuney, M. 1992. Submagmatic microfractures in granites. *Geology* **20**, 35–38.

Bouchez, J.-P., Gleizes, G., Djouadi, T. & Rochette, P. 1990. Microstructure and magnetic susceptibility applied to emplacement kinematics of granites: the example of the Foix pluton (French Pyrenees). *Tectonophysics* **184**, 157–171.

Clemens, J. D. & Mawer, C. K. 1992. Granitic magma transport by fracture propagation. *Tectonophysics* **204**, 339–360.

Cogné, J. P. & Perroud, H. 1988. Anisotropy of magnetic susceptibility as a strain gauge in the Flamanville granite, NW France. *Phys. Earth & Planet. Interiors* **51**, 264–270.

Collinson, D. W. 1983. *Methods in Paleomagnetism and Rock Magnetism*. Chapman and Hall, London.

Colvine, A. C., Fyon, J. A., Heather, K. B., Marmont, S., Smith P. M. & Troop, D. G. 1988. Archean lode gold deposits in Ontario. *Ontario geol. Surv. Misc. Pap.* **139**.

Corfu, F., Jackson, S. L. & R. H. Sutcliffe. 1991. U–Pb ages and tectonic significance of late Archean alkalic magmatism and nonmarine sedimentation: Timiskaming Group, southern Abitibi belt, Ontario. *Can. J. Earth Sci.* **28**, 489–503.

Corfu, F., Krogh, T. E., Kwok, Y. Y. & Jensen, L. S. 1989. U–Pb zircon geochronology in the southwestern Abitibi greenstone belt, Superior Province. *Can. J. Earth Sci.* **26**, 1747–1763.

Cruden, A. R. 1990a. Relative timing of pluton emplacement and fault movement in the Kirkland Lake area, SW Abitibi. In: *Abitibi–Grenville Transect Workshop, Lithoprobe Report* 19. University of British Columbia, 1–4.

Cruden, A. R. 1990b. Flow and fabric development during the diapiric rise of magma. *J. Geol.* **98**, 681–698.

Cruden, A. R. 1991. Syntectonic plutons in the Larder Lake-Cadillac Deformation Zone: Implications for the timing of late Archean deformation in the SW Abitibi Belt. In: *Abitibi–Grenville Transect Workshop, Lithoprobe Report* 25. University of British Columbia, 139–142.

Dimroth, E., Imreh, L., Goulet, N. & Rocheleau, M. 1983a. Evolution of the south-central segment of the Archean Abitibi Belt, Quebec. Part II: Tectonic evolution and geomechanical model. *Can. J. Earth Sci.* **20**, 1355–1373.

Dimroth, E., Imreh, L., Goulet, N. & Rocheleau, M. 1983b. Evolution of the south-central segment of the Archean Abitibi Belt, Quebec. Part III: Plutonic and metamorphic evolution and geotectonic model. *Can. J. Earth Sci.* **20**, 1374–1388.

Dixon, J. M. 1975. Finite strain and progressive deformation in models of diapiric structures. *Tectonophysics* **28**, 89–124.

Ellwood, B. B., Hrouda, F. & Wagner, J.-J. 1988. Symposia on magnetic fabrics: introductory comments. *Phys. Earth & Planet. Interiors* **51**, 249–252.

Ellwood, B. B. & Whitney, J. A. 1980. Magnetic fabric of the Elberton Granite, Northeast Georgia. *J. geophys. Res.* **85**, 1481–1486.

Flinn, D. 1962. On folding during 3-dimensional progressive deformation. *Q. Jl geol. Soc. Lond.* **118**, 385–428.

Gleizes, G. & Bouchez, J.-L. 1991. Le pluton granitique de Bassiés (Pyrénées ariégeoises): zonation, structure et mise en place. *C. r. Acad. Sci. Paris, Sér* II, **312**, 755–762.

Graham, J. W. 1954. Magnetic susceptibility anisotropy, an unexploited petrofabric element. *Bull geol. Soc. Am.* **65**, 1257–1258.

Guillet, P., Bouchez, J.-P. & Wagner J.-J. 1983. Anisotropy of Magnetic Susceptibility and Magmatic Structures in the Guérande Massif (France). *Tectonics* **2**, 419–429.

Gupta, V. K. 1991. Bouger gravity of Ontario, east-central sheet. *Ontario geol. Surv.*, Map 2594, scale 1:1,000,000.

Fernandez, A. 1988. Strain analysis from shape preferred orientation in magmatic rocks. *Bull geol. Instn. Univ. Uppsala* **14**, 61–67.

Hargraves, R. B., Johnson, D. & Chan, C. Y. 1991. Distribution anisotropy: the cause of AMS in igneous rocks? *Geophys Res. Lett.* **18**, 2193–2196.

Henry, B. 1983. Interprétation quantitative de l'anisotropie de susceptibilité magnétique. *Tectonophysics* **91**, 165–177.

Hext, G. R. 1963. The estimation of second-order tensors, with related tests and design. *Biometrica* **50**, 353–373.

Hibbard, M. J. 1986. Deformation of incompletely crystallised magma systems: granitic gneisses and their tectonic implications. *J. Geol.* **95**, 543–561.

Hodgson, C. J. & J. V. Hamilton, 1989. Gold mineralization in the Abitibi greenstone belt: end stage result of Archean collisional tectonics? *Econ. Geol. Monogr.* **6**, 86–100.

Hrouda, F. 1982. Magnetic anisotropy of rocks and its application in geology and geophysics. *Geophys. Surv.* **5**, 37–82.

Hubert, C. 1990. Chronology of incremental deformations across the Larder Lake–Cadillac Tectonic Zone (LCTZ) in the area south of Rouyn-Noranda. In: *Abitibi–Grenville Transect Workshop, Lithoprobe Report* 19. University of British Columbia, 5–7.

Ildefonse, B. & Fernandez, A. 1988. Influence of the concentration of rigid markers in a viscous medium on the production of preferred orientation. An experimental contribution, 1. Non-coaxial strain. *Bull geol. Instn. Univ. Uppsala* **14**, 55–66.

Ildefonse, B., Launeau, P., Bouchez, J.-L. & Fernandez, A. 1992. Effect of mechanical interactions on the development of shape preferred orientations: a two-dimensional experimental approach. *J. Struct. Geol.* **14**, 73–83.

Jackson, S. L. & Fyon, J. A. 1991. The western Abitibi Subprovince in Ontario. In: *Geology of Ontario. Ontario geol. Surv. Spec. Vol.* **4**, 405–482.

Jackson, S. L., Sutcliffe, R. H., Ludden, J. N., Hubert, C., Green, A. G., Milkereit, B., Mayrand, L., West, G. F. & Verpaelst, P. 1990. Southern Abitibi Greenstone Belt: Archean crustal structure from seismic reflection profiles. *Geology* **18**, 1086–1090.

Jelinek, V. 1978. Statistical processing of anisotropy of magnetic susceptibility measured on groups of specimens. *Studia geoph. geod.* **22**, 50–62.

Jelinek, V. 1981. Characterization of the magnetic fabrics of rocks. *Tectonophysics* **79**, T63–T67.

Jensen, L. S. 1985. Synoptic mapping of the Kirkland Lake–Larder Lake areas, district of Timiskaming. *Ontario geol. Surv. Misc. Pap.* **126**, 112–120.

Jolly, W. T. 1978. Metamorphic history of the Archean Abitibi Belt. *Geol. Surv. Can. Pap.* **78-10**, 63–78.

King, R. F. 1966. The magnetic susceptibility of some Irish granites. *Geol. J.* **5**, 43–66.

Launeau, P. 1990. Analyse numérique des images et orientations préférentielles de forme des agrégats polyphasés: application á l'analyse cinématique des granites. Unpublished Thèse de Doctorat, Université de Toulouse.

Launeau, P. & Bouchez, J.-L. 1992. Mode et orientation préférentielle de forme des granites par analyse d'images numériques. *Bull. Soc. geol. Fr.* **163**, 721–732.

Launeau, P., Bouchez, J.-L. & Benn, K. 1990. Shape preferred orientation of object populations: automatic analysis of digitized images. *Tectonophysics* **180**, 201–211.

Lawton, K. D. 1957. Geology of Boston Township and part of Pacaud Township. *Ontario Dept Mines Annu. Rep.* **66**, Pt 5, 1–53.

Levesque, G. S., Cameron, E. M. & Lalonde, A. E. 1991. Duality of magmatism along the Kirkland Lake-Larder Lake fault zone, Ontario. *Geol. Surv. Can. Pap.* **91-1C**, 17–24.

Lister, J. R. & Kerr, R. C. 1991. Fluid-mechanical models of crack propagation and their application to magma transport in dykes. *J. geophys. Res.* **B96**, 10,049–10,077.

Ludden, J., Hubert, C. & Gariepy, C. 1986. The tectonic evolution of the Abitibi greenstone belt of Canada. *Geol. Mag.* **123**, 153–166.

MacLean, A. 1956. Geology of Lebel Township. *Bull. Ontario Dept Mines* **150**.

Mahon, K. I., Harrison, T. M. & Drew, D. A. 1988. Ascent of a granitoid diapir in a temperature varying medium. *J. geophys. Res.* **B93**, 1174–1188.

Mueller, W. & Davidson, J. A. 1991. Tectonic and volcanic influences on sedimentation: the Kirkland Basin. In: *Abitibi–Grenville Transect Workshop, Lithoprobe Report* 25. University of British Columbia, 151–153.

Nicolas, A. 1992. Kinematics in magmatic rocks with special reference to gabbros. *J. Petrol.* **33**, 891–915.

Nicolas, A., Freydier, C., Godard, M. & Vauchez, A. 1993. Magma chambers at ocean ridges: how large? *Geology* **21**, 53–56.

Nye, J. F. 1985. *Physical Properties of Crystals.* Oxford University Press, New York.

Owens, W. H. 1974. Mathematical model studies on factors affecting the magnetic anisotropy of deformed rocks. *Tectonophysics* **24**, 115–131.

Paterson, S. R. & Fowler, T. K. Jr. 1993. Re-examining pluton emplacement processes. *J. Struct. Geol.* **15**, 191–206.

Paterson, S. R., Vernon, R. H. & Tobisch, O. T. 1989. A review of the criteria for the identification of magmatic and tectonic foliations in granitoids. *J. Struct. Geol.* **11**, 349–363.

Rathore, J. S. & Kafafy, A. M. 1986. A magnetic fabric study of the Shap region in the English Lake District. *J. Struct. Geol.* **8**, 69–77.

Robert, F. 1989. Internal structure of the Cadillac tectonic zone southeast of Val d'Or, Abitibi greenstone belt, Quebec. *Can. J. Earth Sci.* **26**, 2661–2675.

Robin, P.-Y. F. & Cruden A. R. 1991. Strain fabric patterns in ideally ductile transpressive zones and in a possible Archean prototype: the Larder Lake Break. *Geol. Soc. Am. Ab. w. Prog.* **23**, A177.

Rochette, P. 1987. Magnetic susceptibility of the rock matrix related to magnetic fabric studies. *J. Struct. Geol.* **9**, 1015–1020.

Rowins, S. M., Lalonde, A. E. & Cameron, E. M. 1991. Magmatic oxidation in the syenitic Murdoch Creek intrusion, Kirkland Lake, Ontario: evidence from the ferromagnesian silicates. *J. Geol.* **99**, 395–414.

Stacey, F. D. 1960. Magnetic anisotropy of igneous rocks. *J. geophys. Res.* **65**, 2429–2442.

Sutcliffe, R. H., Smith, A., Doherty, W. & Barnett, R. L. 1990. Mantle derivation of Archean amphibole bearing granitoid and associated mafic rocks: evidence from the southern Superior Province, Canada. *Contr. Miner. Petrol.* **105**, 255–274.

Toogood, D. J. & Hodgson, C. J. 1986. Relationship between gold deposits and the tectonic framework of the Abitibi greenstone belt in the Kirkland Lake–Larder Lake area. *Ontario geol. Surv. Misc. Pap.* **130**, 4–15.

Uyeda, S., Fuller, M. D., Belshe, J. C. & Girdler, R. W. 1963. Anisotropy of magnetic susceptibility of rocks and minerals. *J. geophys. Res.* **68**, 279–291.

Van der Molen, I. & Paterson, M. S. 1979. Experimental deformation of partially melted granite. *Contr. Miner. Petrol.* **70**, 299–318.

Van der Voo, R. & Klootwijk, C. T. 1972. Paleomagnetic reconnaissance study of the Flamanville granite, with special reference to the anisotropy of its susceptibility. *Geol. Mijnb.* **51**, 609–617.

Windley, B. F. 1984. *The Evolving Continents* (2nd edn). John Wiley & Sons, New York.